

Quasi-Scarred Resonances in Chaotic Microdisk Cavity

Soo-Young Lee, Sunghwan Rim, Jung-Wan Ryu, Tae-Yoon Kwon, Muhan Choi, and Chil-Min Kim
*National Creative Research Initiative Center for Controlling Optical Chaos,
 Pai-Chai University, Daejeon 302-735, Korea*

We study resonance patterns of a chaotic microcavity. It is shown that the scar theory of billiard systems should be modified to be applied to dielectric cavity so that strongly localized resonances with no exact underlying periodic orbit, we call these quasi-scarred resonances, can appear. We explain the formation of quasi-scarred patterns in consideration of uncertainty and interference properties. We also discuss relationships between quasi-scarred resonances and the steady probability distribution developed in ray dynamics.

PACS numbers: 05.45.Mt, 42.55.Sa

Since the seminal finding of scarred eigenfunctions in a chaotic stadium billiard by Heller[1], many authors have studied this abnormal phenomenon both theoretically[1, 2, 3] and experimentally[4, 5, 6] to understand the impact of classical periodic orbits in various chaotic systems. In general, statistics of quantum mechanical eigenvalues and eigenfunctions of classically chaotic systems can be well described by Random Matrix Theory (RMT)[7]. From the viewpoint of RMT the existence of scarred eigenfunctions, which show enhanced amplitude along an unstable periodic orbit, cannot be justified. The scar phenomenon would, therefore, be regarded as the first correction on RMT containing specific informations of the chaotic system concerned[8, 9].

Recently, there are several reports of observation of scarred lasing modes in dielectric microcavities of various boundary shapes[10, 11, 12, 13]. In the papers authors have identified the scarred lasing modes by matching the directionality of lasing emission and possible unstable periodic orbit in the chaotic microcavities. We note that none of the papers has developed appropriate modification of the scar theory of hamiltonian chaotic systems. Basically, dielectric microcavities have quite different classical dynamics compared with that of billiard systems. First, it is a dissipative system, i.e., the energy confined in cavity is a decreasing function of time and the energy loss corresponds to the escaping energy by emission. Second, the refractive index n plays a crucial role in characterizing ray dynamics in the microcavities, e.g., it determines the critical angle of total internal reflection, $\theta_c = \arcsin(1/n)$, and θ_c is, in turn, closely related to directionality of rays on the boundary. We note that these inherent characteristics of dielectric cavities can give rise to important and enormous differences in resonance patterns.

In this Letter, we investigate ray dynamical and wave dynamical properties of a classically chaotic dielectric microcavity, spiral-shaped microdisk. In the ray dynamical analysis we define *steady probability distribution* $P_s(s, p)$, where s is the arc length of the boundary and $p = \sin \theta$, θ being incident angle, i.e., (s, p) is the Birkhoff coordinates. The existence of $P_s(s, p)$ explains exponential decay behaviors of the energy $\mathcal{E}(t)$ confined in the microdisk

and *escape time distribution* $P_{es}(t)$ at $t > t_c$, where t_c is the critical time at which steady behavior begins to occur in $P_{es}(t)$ (see Fig.1). In the wave dynamical analysis, we obtain patterns of resonances around $\text{Re}(nkR) \simeq 110$, and find out that more than half of resonances show localized patterns, and the basic shapes of the patterns are triangle and star for $n = 2$ and 3, respectively. The localized resonances look like scarred eigenfunctions in billiard systems, but it is evident that this scar-like resonance patterns are not supported by any periodic orbit. We call these *quasi-scarred* resonances. We will show that these quasi-scarred resonances are closely related to the steady probability distribution $P_s(s, p)$, and the formation of the quasi-scarred pattern can be understood in consideration of uncertainty and interference properties of waves. Moreover, the quasi-scarred resonances are responsible for very strong directional lasing emission.

The spiral-shaped microdisk has been introduced by Chern et al.[14] to generate unidirectional lasing emission, and the boundary shape is given by

$$r(\phi) = R(1 + \frac{\epsilon}{2\pi}\phi) \quad (1)$$

in polar coordinates (r, ϕ) , where R is the radius of the spiral at $\phi = 0$ and ϵ is the deformation parameter, we set $\epsilon = 0.1$ and $R = 1$ throughout this Letter. The classical dynamics of this spiral-shaped billiard is chaotic, a trajectory starting from an arbitrary initial point (s_0, p_0) fills evenly the whole phase space (s, p) . Therefore most of the eigenfunctions of this billiard would show highly irregular patterns and evenly distributed amplitude inside the billiard except small number of eigenfunctions scarred mainly by the least unstable periodic orbit of the system.

However, the dielectric microdisk of this boundary shape is a dissipative system, i.e., ray trajectories cannot survive arbitrary long time due to energy loss by emission, and the related time scale depends on initial point (s_0, p_0) . To illustrate this dissipative property we consider *survival probability distribution* $\tilde{P}(s, p, t)$, and $\int ds dp \tilde{P}(s, p, t) \leq 1$ due to energy loss by emission from the cavity. The confined energy and escape time distribution can then be described by

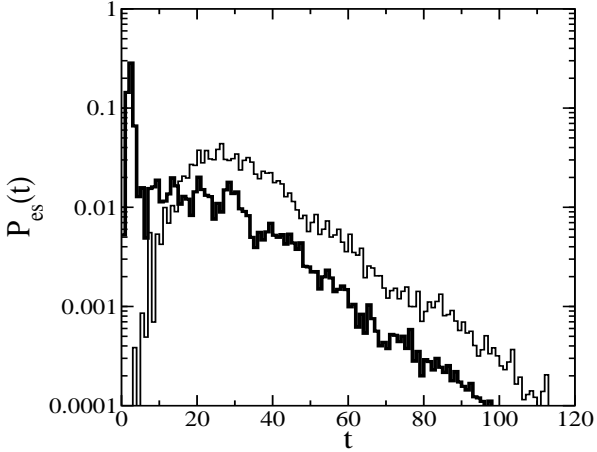


FIG. 1: The escape time distributions $P_{es}(t)$ with $n = 2$ for two different sets of initial points; the thick and thin lines represent numerical results for Set A and Set B, respectively. The time t is scaled to be the length of ray trajectory when $R = 1$.

$$\mathcal{E}(t) = \mathcal{E}_0 \int ds dp \tilde{P}(s, p, t), \quad (2)$$

$$P_{es}(t) = \int ds dp \tilde{P}(s, p, t) \mathcal{T}(p), \quad (3)$$

where $\mathcal{T}(p)$ is the transmission coefficient, which has nonzero value in the range of $-p_c < p < p_c$ ($p_c = \sin \theta_c$), given by Fresnel's equation[15]. We note the fact that the initial energy is the sum of confined energy and escaped energy, then

$$\frac{d\mathcal{E}(t)}{dt} = -\mathcal{E}_0 P_{es}(t). \quad (4)$$

The above equations are generally satisfied by construction.

Consider a set of initial points which are uniformly distributed in the phase space (s, p) . We can imagine several channels C_i through which ray trajectories suffer energy loss by emission, and for each channel we can designate effective decay rates γ_i , where i is the channel index, and let γ_0 be the smallest one for convenience. For short time range, all channels would contribute to total energy loss, but shortly after, the channel with maximum decay rate would stop to contribute as long as there is no continuous and intense inflow from other parts of the phase space. Through the same mechanism other channels start to close, and eventually at $t > t_c$ only the channel C_0 with γ_0 would contribute to total energy loss, and the survival probability distribution $\tilde{P}(s, p, t)$ would show a steady behavior. We assume that there is steady probability distribution $P_s(s, p)$ such that

$$\tilde{P}(s, p, t) = B(t) P_s(s, p). \quad (5)$$

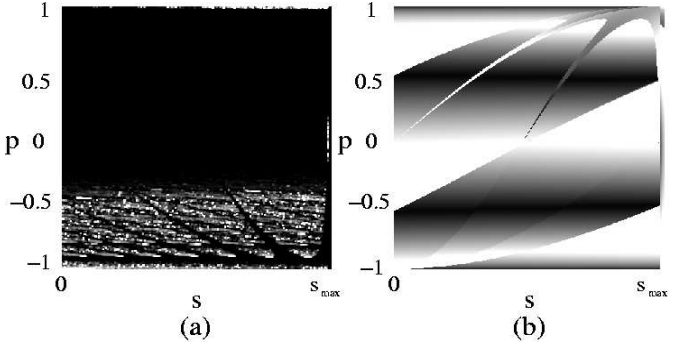


FIG. 2: (a) The normalized survival probability distribution $\tilde{P}(s, p, t)$ sampled in the time range of $57 < t < 60$ for Set A. (b) Distribution of distance d in phase space after three bounces. In figures darker regions correspond to lower amplitude.

Substituting Eq.(5) into Eqs.(2), (3) and, in turn, into Eq.(4), we can obtain $B(t) = A \exp(-\gamma_0 t)$ where A is a constant. The smallest decay rate γ_0 is given by

$$\gamma_0 = \int ds dp P_s(s, p) \mathcal{T}(p). \quad (6)$$

We get, therefore, $\mathcal{E}(t) = \mathcal{E}_0 A \exp(-\gamma_0 t)$ and $P_{es}(t) = \gamma_0 A \exp(-\gamma_0 t)$ for $t > t_c$.

For simplicity's sake, we will concentrate on TE (transverse electric) mode throughout this Letter. In Fig.1, the escape time distributions $P_{es}(t)$ are shown for $n = 2$ case. We consider two different sets of 400×400 initial points, one is the uniformly distributed set over the whole phase space (Set A) and the other is the uniformly distributed one in a part of the phase space, $(0 < s < s_{max}/2, 0.5 < p < 0.75)$ (Set B), where s_{max} is the total length of the boundary. Note that above $t_c \simeq 30$ exponential decay behaviors are shown. The slope of the linear part determines the decay rate γ_0 . The similar slopes for both Set A and Set B reflect that rays lose their energy through the same channel, i.e., C_0 . The details of the channel C_0 will appear in the structure of the steady probability distribution $P_s(s, p)$.

Figure 2 (a) shows an approximate steady probability distributions $P_s(s, p)$ for $n = 2$ given by normalizing the survival probability distribution $\tilde{P}(s, p, t)$ in the time range of $57 < t < 60$ for Set A. The structure of the approximate $P_s(s, p)$ is almost invariant in other time ranges of the linear part ($t > t_c$) and even for Set B. It is clear that the main contribution to energy loss comes from tangential emissions just above the critical line ($-p_c = -1/2$). So, we can see that the channel C_0 is the way that the ray trajectories first rotate counter clockwise ($p > p_c$), and change their rotational direction by reflection on the notch part, and afterwards gradually approach to $-p_c$, and the main part of them are eventually emitted out from the microdisk cavity and the remain repeat the same process. The distribution limited in negative value of p means strong chirality of this

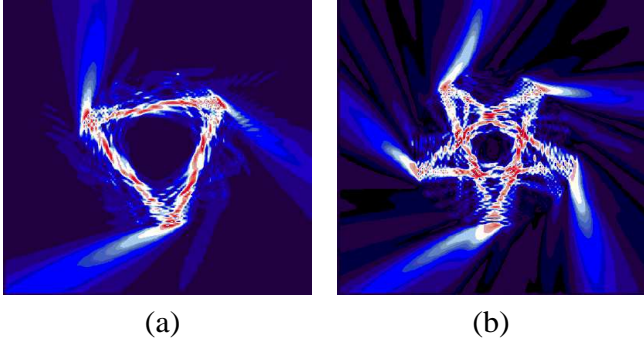


FIG. 3: (color) Quasi-scarred resonances in spiral-shaped microdisk cavity. (a) $n = 2$ and $nkR = (109.695, -0.1125)$. (b) $n = 3$ and $nkR = (109.595, -0.1158)$.

spiral-shaped microdisk. The spike structure in Fig.2 (a) implies missing of the trajectories reflected with $|p| > p_c$ at the notch. This structure would give important informations about statistical properties of resonances, i.e., far field and near field distribution of resonances would show minima at values corresponding to the missing trajectories.

More direct implication on resonance patterns can arises from the distribution of resulting distance after 3 bounces (Fig.2(b)), i.e., $d = (s_f - s_i)^2 + (p_f - p_i)^2$ where (s_i, p_i) is the initial position and (s_f, p_f) being the position after 3 bounces. We note that in Fig.2 (b) the critical line $p = -p_c$ lies on the dark region representing the initial positions with short distance d . Since the rays in the region just above $-p_c$ are partially emitted out, the remaining reflected rays would make rough triangle. As discussed later, the imprint of this fact appears apparently in resonance patterns (see Fig.3 (a)). Although $n = 3$ case is not presented in figures, the distance distribution after 5 bounces also shows similar features, implying that star shape ray trajectories would be responsible for resonance patterns (see Fig.3 (b)).

Using the boundary element method[16], we obtain resonances around $\text{Re}(nkR) \simeq 110$ for the spiral-shaped dielectric microdisk, 24 resonances for $n = 2$ and 23 resonances for $n = 3$. For $n = 2$ the imaginary values $\text{Im}(nkR)$ of resonances are distributed over the range of $-0.5 < \text{Im}(nkR) < -0.05$ and many resonances (about 18 resonances) are located near $\text{Im}(nkR) \simeq -0.1$. For $n = 3$ most of the resonances are scattered over the range of $-0.3 < \text{Im}(nkR) < -0.1$. From the resonances we find an important fact that the basic localized structures of the resonance patterns are triangular and star shapes for $n = 2$ and 3, respectively, which is consistent with the implication of $P_s(s, p)$. More interestingly, these basic structures appear in most of the resonances. Some of these resonances look like strongly scarred eigenfunctions of billiard system, showing strong directional emissions matched to the triangular and star patterns. The nkR values and patterns for whole resonances will be presented elsewhere due to space limit of this Letter.

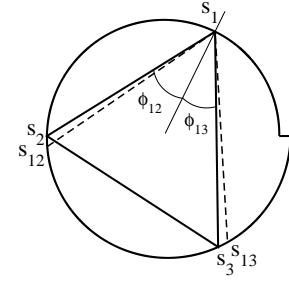


FIG. 4: Schematic diagram for quantifying the degree of uncertainty. The trajectory satisfying Snell's law, with an incident angle $(\phi_{12} + \phi_{13})/2$, is denoted by dashed lines.

In Fig.3 the most clearly localized resonances for $n = 2$ and 3 are shown. The patterns look like strongly scarred resonances, but there is no exact underlying unstable periodic orbit. Absence of periodic orbits of simple geometry, e.g., triangle and star, is evident by numerical evaluation of $\delta p = p_i - p_f$ for closed triangle or star trajectory starting from (s_i, p_i) and terminating at (s_i, p_f) . We obtain $|\delta p| > \sigma$, σ is a positive constant, for arbitrary s_i value. Since the localized patterns of resonances are not supported by any unstable periodic orbit, we call these *quasi-scarred resonances*. The existence of quasi-scarred resonances in dielectric cavities can be understood from the inherent property of dissipative systems, uncertainty characteristics. Another important result from the resonance pattern analysis is that many resonances are quasi-scarred, e.g., in the present case more than half are quasi-scarred, while only small fraction of eigenfunctions are scarred in billiard systems. This fact would also be true for scarred resonances in other dielectric cavities and, in practical experiment, this is so crucial that the quasi-scarred (scarred) lasing emission can be excited easily due to its dominant existence in resonances.

Now, we consider bouncing positions of the triangle formed in quasi-scarred resonances which seem to have definite dependence on their $\text{Re}(nkR)$ values. We assume that the triangle in quasi-scarred resonances would have minimum deviation from the ray trajectory governed by Snell's law, and gives maximum constructive interference under constraint of high intensity of electric field at the bouncing positions. We quantify these by two factors, α and β as followings. Let s_i ($i = 1, 2, 3$) be the bouncing positions of a triangle, from the angles (ϕ_{ij}, ϕ_{ik}) to the normal line on the boundary, we can define $p_{ij} = \sin(\phi_{ij})$, $p_{ik} = \sin(\phi_{ik})$, and $p_i = \sin(\frac{\phi_{ij} + \phi_{ik}}{2})$ (here i, j, k are cyclic). Also we get the new positions s_{ij}, s_{ik} as the next positions of (s_i, p_i) and $(s_i, -p_i)$, respectively (see Fig.4). Then we define partial uncertainty of the triangle given by (s_1, s_2, s_3) as

$$\alpha_i = [(p_i - p_{ij})(s_j - s_{ij})]^2 + [(p_i - p_{ik})(s_k - s_{ik})]^2. \quad (7)$$

Total uncertainty, therefore, is the sum of these terms,

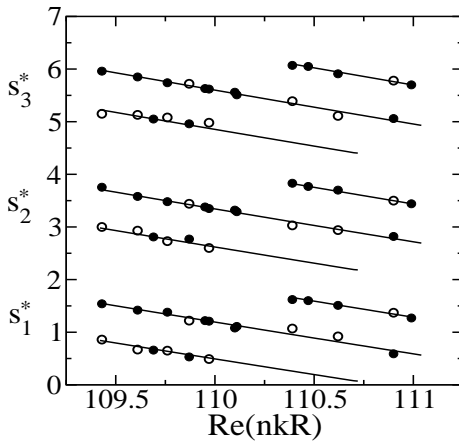


FIG. 5: Variation of the optimized bouncing positions (s_1^*, s_2^*, s_3^*) . The solid lines denote the present theory with a correction $\mu = 0.06$. The circles represent the bouncing positions of triangular quasi-scarred resonance patterns of $n = 2$ case; three solid circles correspond to the main triangle pattern, and three open circles do to the secondary triangle pattern in a quasi-scarred resonance.

$\alpha = \sum_{i=1}^3 \alpha_i$. By definition, when the triangle is a periodic orbit, α becomes zero. To quantify the degree of constructive interference we consider $m_i + \beta_i = l_i/(\lambda/2) + \delta\phi/\pi$ for each triangle segment of length l_i , where m_i is an integer and $-0.5 < \beta_i < 0.5$, $\lambda = 2\pi/(nk)$, and $\delta\phi$ is the phase shift arised from total internal reflection[17]. Total quantity for the degree of constructive interference is then $\beta = \sum_{i=1}^3 \beta_i^2$ with an additional constraint that the sum $M = \sum_{i=1}^3 m_i$ should be even.

We first determine triangles with minimum uncertainty

α as a function of s_1 , and then apply the condition of minimum β to the triangles. From this process we get the most optimized triangle of (s_1^*, s_2^*, s_3^*) for a fixed $\text{Re}(nkR)$. The direct application of this method shows systematic deviation from bouncing positions of resonance patterns. This systematic discrepancy comes from the fact that rays inside microdisk cavity have angular distribution and, also the boundary has curvature, which gives arise to a correction of the Snell's law. This effect is larger near the critical angle θ_c , and partially studied and known as Goos-Hänchen[18] and Fresnel Filtering effects[12, 19]. We here incorporate these effects by taking effective segment length $l_i^* = l_i + \mu\lambda$. The results are shown in Fig.5. The solid lines are results of the present theory with $\mu = 0.06$ which show very good agreement with the bouncing positions (denoted by circles) of the quasi-scarred resonances. Absence of bouncing positions near $s = 2$ and 4.5 is consistent with the spike structure of the approximate steady probability distribution $P_s(s, p)$ in Fig.2 (a).

In conclusion, we have found that the localized patterns of resonances in spiral-shaped dielectric microdisk cavity can be understood by introducing quasi-scarred phenomenon which has not reported so far in other dielectric cavities. Unlike scarred eigenfunctions of billiard systems, large fraction of resonances are quasi-scarred, which would be also true for scarred resonances. The patterns of quasi-scarred resonances are expected from the steady probability distribution $P_s(s, p)$ and more precisely determined in consideration of uncertainty and interference effect of waves.

This work is supported by Creative Research Initiatives of the Korean Ministry of Science and Technology.

[1] E. J. Heller, Phys. Rev. Lett. **53**, 1515 (1984).
[2] E. B. Bogomolny, Physica **D 31**, 169 (1988).
[3] M. V. Berry, Proc. Roy. Soc. **A 243**, 219 (1989).
[4] S. Sridhar, Phys. Rev. Lett. **67**, 785 (1991).
[5] J. Stein and H.-J. Stöckmann, Phys. Rev. Lett. **68**, 2867 (1992).
[6] T. M. Fromhold, P. B. Wilkinson, F. W. Sheard, L. Eaves, J. Miao, and G. Edwards, Phys. Rev. Lett. **75**, 1142 (1995); P. B. Wilkinson, T. M. Fromhold, L. Eaves, F. W. Sheard, N. Miura, and T. Takamasu, Nature **380**, 608 (1996).
[7] O. Bohigas, M. J. Giannoni, and C. Schmit, Phys. Rev. Lett. **52**, 1 (1984).
[8] L. Kaplan, Phys. Rev. Lett. **80**, 2582 (1998); L. Kaplan and E. J. Heller, Ann. Phys. **264**, 171 (1998); L. Kaplan, Nonlinearity **12**, R1 (1999).
[9] S. C. Creagh, S.-Y. Lee, and N. D. Whelan, Ann. Phys. **295**, 194 (2002); S.-Y. Lee and S. C. Creagh, Ann. Phys. **307**, 392 (2003).
[10] S.-B. Lee, J.-H. Lee, J.-S. Chang, H.-J. Moon, S. W. Kim, and K. An, Phys. Rev. Lett. **88**, 033903 (2002).
[11] C. Gmachl, E. E. Narimanov, F. Capasso, J. N. Bala-
largeon, and A. Y. Cho, Opt. Lett. **27**, 824 (2002).
[12] N. B. Rex, H. E. Tureci, H. G. L. Schwefel, R. K. Chang, and A. D. Stone, Phys. Rev. Lett. **88**, 094102 (2002).
[13] T. Harayama, T. Fukushima, P. Davis, P. O. Vaccaro, T. Miyasaka, T. Nishimura, and T. Aida, Phys. Rev. E **67**, 015207(R) (2003).
[14] G. D. Chern, H. E. Tureci, A. D. Stone, R. K. Chang, M. Kneissl, and N. M. Johnson, Appl. Phys. Lett. **83**, 1710 (2003).
[15] J. Hawkes and I. Latimer, *Lasers: Theory and Practice* (Prentice Hall, 1995).
[16] J. Wiersig, J. Opt. A: Pure Appl. Opt. **5**, 53 (2003).
[17] G. R. Fowles, *Introduction to Modern Optics* (Holt, Rinehart and Winston, 1975).
[18] F. Goos and H. Hänchen, Ann. Phys. (Leipzig) **1**, 333 (1947); M. Hentschel and H. Schomerus, Phys. Rev. E **65**, 045603(R) (2002).
[19] H. E. Tureci and A. D. Stone, Opt. Lett. **27**, 7 (2002).